EPSC Abstracts
Vol. 6, EPSC-DPS2011-136, 2011
EPSC-DPS Joint Meeting 2011

Insolation on Exoplanets with Eccentricity and Obliquity

A. R. Dobrovolskis
Lick Observatory, University of California, Santa Cruz, USA (anthony.r.dobrovolskis@nasa.gov / Fax: 1-650-6779)

1. Introduction

Spin-orbit resonances, where a planet's orbital period is an integer or half-odd integer multiple of its rotation period, can have profound effects on the distribution of insolation over a planet's surface, protecting certain regions from the worst extremes of radiation and temperature. This has implications for the detection and interpretation of thermal emissions from extrasolar planets, as well as for their habitability.

2. Global Patterns

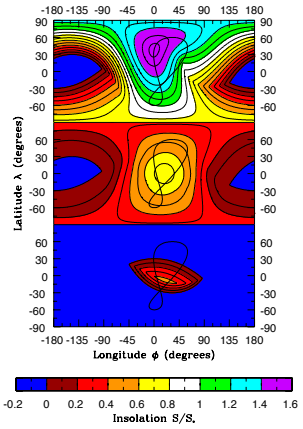

Figure 1: Insolation for the case of synchronous rotation, with $\alpha = 45°$, $\beta = 60°$, and $e = 0.20$. Top panel: maximum insolation $\hat{S}$, peaking at 1.5625 S_*. Middle panel: mean insolation $\bar{S}$, peaking at 0.7350 S_*. Bottom panel: minimum insolation $\check{S}$, peaking at 0.4482 S_*. Contours: S/S_* = 0, .10, .20, .30, .40, .50, .60, .70, .80, .90, 1.00, 1.10, 1.20, 1.30, 1.40, 1.50, and 1.55. The heavy black figure-8 curve in each panel shows the ground track of the sub-stellar point.

Previously I described the insolation patterns on exoplanets in synchronous rotation, or in other spin-orbit resonances; Dobrovolskis (2007) considered finite orbital eccentricities e, but obliquities β of zero (or 180°), while Dobrovolskis (2009) treated arbitrary β, but zero e . Here I consider spin-orbit resonances for both finite e and β together.

The simultaneous presence of nonzero e and β requires the introduction of another parameter α, the longitude of vernal equinox (relative to periapsis). Insolation patterns depend in complicated and non-separable ways on α, β, e, latitude, longitude, time, and the planet's rotation rate ω.

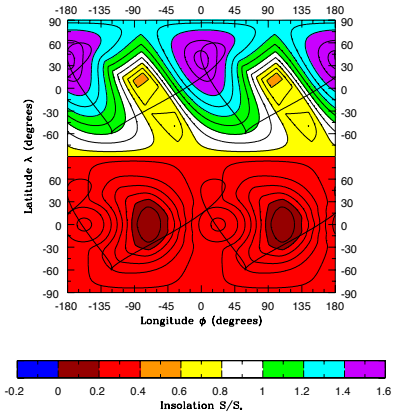

Figure 2: Insolation for the 3/2 spin-orbit resonance, with $\alpha = 45°$, $\beta = 60°$, and $e = 0.20$. Top panel: maximum insolation $\hat{S}$, with maxima of 1.5625 S_* and minima of 0.5369 S_*. Contours: S/S_* = .60, .70, .80, .90, 1.00, 1.10, 1.20, 1.30, 1.40, 1.50, and 1.55. Bottom panel: mean insolation $\bar{S}$, with maxima of 0.3234 S_* and minima of 0.1646 S_*. Contours: S/S_* = .18, .20, .22, .24, .26, .28, .30, and .32. The heavy black curve in each panel shows the ground track of the sub-stellar point.

For instance, Fig. 1 shows the maximum insolation $\hat{S}$, the minimum insolation $\check{S}$, and the time-averaged insolation $\bar{S}$ for a synchronously spinning planet with $e = 0.20$, $\beta = 60°$, and $\alpha = 45°$; *cf.* Fig. 8 of Dobrovolskis (2009). All of these have been normalized by the "extra-solar constant" $S_* \equiv L^*/(4\pi a^2)$, where L^* is the luminosity of the star, and a is the semi-major axis of the planet's orbit.

Note the blue region of eternal night in the top and middle panels of Fig. 1, and the non-blue region of perpetual daylight in its bottom panel. Other spin-orbit resonances do not share these particular features, but still display a kaleidoscopic variety of complicated insolation patterns.

As an example, Fig. 2 displays $\hat{S}$ and $\bar{S}$ for the same parameters as Fig. 1, but for the case where the planet rotates three times during two orbits, like Mercury ($\check{S}$ is not shown because it vanishes for non-synchronous rotations). Resonances like this one, where the planet's orbital period is a half-odd multiple of its rotation period, produce identical insolation patterns at longitudes $180°$ apart, as seen in Fig. 2.

Furthermore, all such resonances display an entirely unexpected symmetry of $\bar{S}$ about their equators, as seen in the lower panel of Fig. 2. This suprising symmetry arises *regardless* of α, β, or e, but is not shared either by $\hat{S}$ (upper panel) or by the ground track of the sub-stellar point (heavy black curves), and does not occur for integer period ratios, either odd or even.

3. Polar Insolation

The insolation problem becomes much simpler when restricted to the planet's rotational poles, which can play an important role in determining global climate. This supresses not only latitude and longitude, but ω too, so that the following applies to any non-resonant rotation as well as to all of the spin-orbit resonances.

Of course $\check{S}$ vanishes at both poles, while

$$\bar{S} = \frac{S_* \sin\beta}{\pi\sqrt{1-e^2}} \qquad (1)$$

at each pole, independent of α! $\hat{S}$ also is proportional to $\sin\beta$, but generally differs at the two poles, and still depends on both e and α in a complicated, non-separable manner.

Figure 3 displays this dependence for the "north" pole; the corresponding plot for the "south" pole would be the reflection of Fig. 3 through its horizontal axis h=0. Note that Fig. 3 is symmetric about its vertical axis k=0.

The difference in insolation between the poles also can be an important determiner of climate. A similar analysis as in Fig. 3 reveals that the ratio of $\hat{S}$ at the north pole to $\hat{S}$ at the south pole approaches a maximum of 27 as e approaches 1 and α approaches $90°$ (and a minimum of 1/27 as α approaches $-90°$).

4. Summary and Conclusions

The simultaneous presence of eccentricity and obliquity leads to complicated and unexpected insolation patterns on extrasolar planets in spin-orbit resonance, but restricting attention to the planets' poles simplifies the situation considerably.

References

Dobrovolskis, A. R. : Spin states and climates of eccentric exoplanets, Icarus, Vol. 192, pp. 1–23, 2007.

Dobrovolskis, A. R. : Insolation patterns on synchronous exoplanets with obliquity, Icarus, Vol. 204, pp. 1–10, 2009.

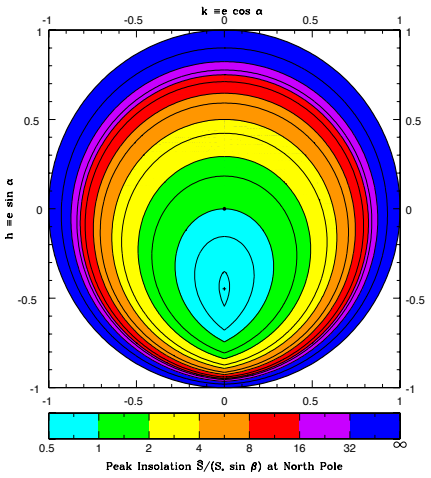

Figure 3: Peak insolation $\hat{S}$ at the north pole (normalized by $S_* \sin\beta$), as a function of polar coordinates e and α, or of rectangular coordinates h and k. Contours: 0.55, 0.75, 1.0, 1.5, 2, 3, 4, 6, 8, 12, 16, 20, 32, 100, and ∞. The asterisk through the unit contour denotes the origin $e = 0$, while the + denotes the minimum of $\hat{S}$.